Supporting Information

Accelerating electrochemical performance of solid oxide fuel cells using a Ce(Gd, Bi, Yb)$O_{2-\delta}$ diffusion barrier layer acting as an oxygen reservoir at high-current loading condition

Hye Young Kim, [a,b] Sang Won Lee, [a,c] Seokhee Lee, [a] Younki Lee, *[b] Ji Haeng Yu *[d] and Tae Ho Shin*[a]

[a] Korea Institute of Ceramic Engineering and Technology, Jinju-si, Gyeongsangnam-do 52851, Republic of Korea

[b] Gyeongsang National University, Jinju-si, Gyeongsangnam-do 52828, Republic of Korea

[c] Department of Chemical and Biomolecular Engineering, Yonsei University, Seoul, 03722, Republic of Korea

[d] Korea Institute of Energy Research, Daejeon, 34101, Republic of Korea

AUTHOR INFORMATION

Corresponding Authors

*E-mail: the@kicet.re.kr (T.H. Shin), jhyu@kier.re.kr (J.H. Yu), ylee@gnu.ac.kr (Y. Lee)

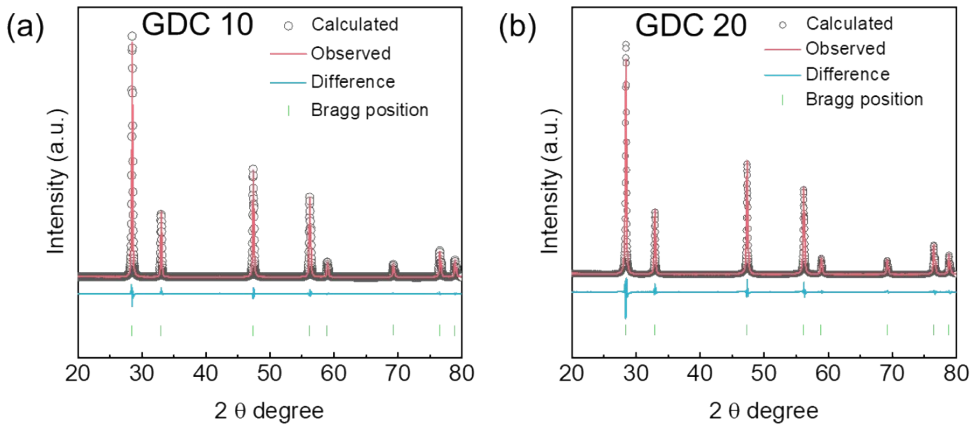

Fig. S1 Rietveld refinement results from X-ray diffraction patterns of (a) GDC 10 and (b) GDC 20. Rietveld refinement results confirmed that both GDC 10 and GDC 20 possess a cubic structure with the space group Fm-3m. The lattice parameters were determined to be 5.4203(3) Å and 5.4252(3) Å for GDC 10 and GDC 20, respectively. The increase in the lattice parameter with higher Gd doping is attributed to the larger ionic radius of Gd^{3+} (1.07 Å) compared to Ce^{4+}(0.97 Å).

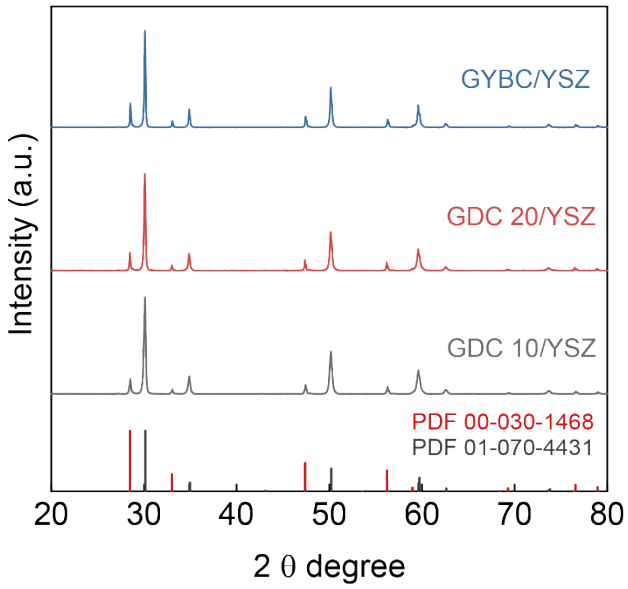

Fig. S2 X-ray diffraction patterns GDC 10/YSZ, GDC 20/YSZ, and GYBC/YSZ powder after sintering at 1250 °C 2h. X-ray diffraction (XRD) analysis was conducted to investigate the reactivity between the electrolyte YSZ and the doped ceria materials (GDC 10, GDC 20, and GYBC). Previous studies have reported that GDC and YSZ do not react at 1250°C. Similarly, our results show no evidence of a reaction between GYBC and YSZ, indicating good chemical compatibility between the two materials.

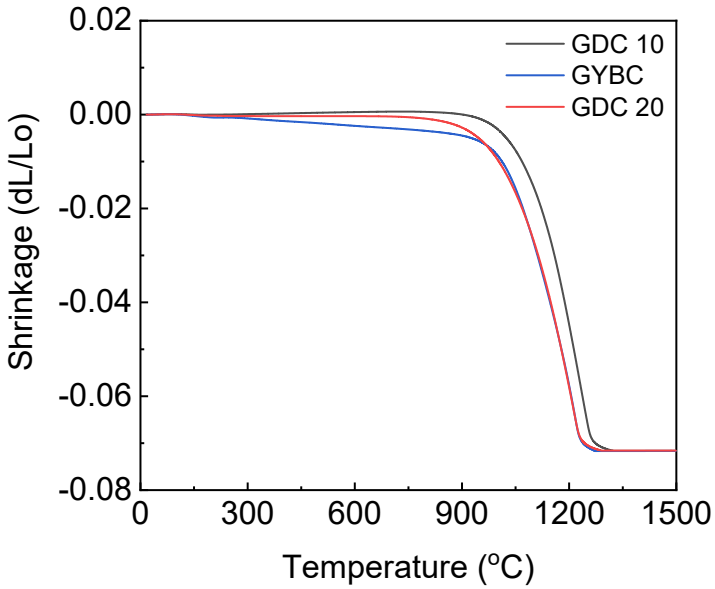

Fig. S3 Shrinkage behavior of GDC 10, GDC 20, and GYBC with temperature. The shrinkage of each pellets could be observed up to 1500 °C. The GYBC starts to shrink at a lower temperature.

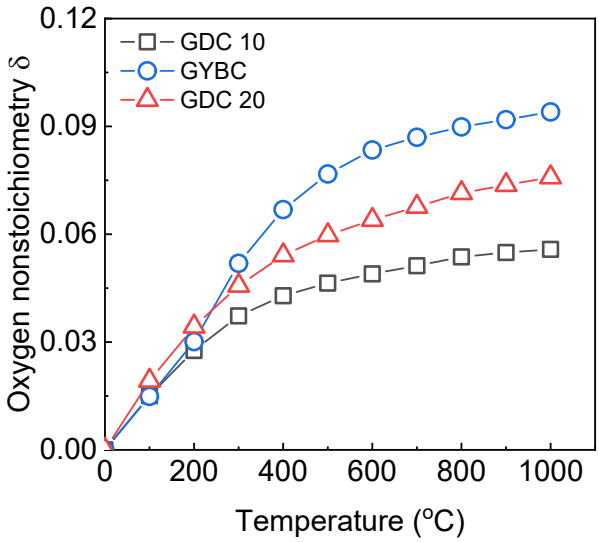

Fig. S4 Estimated oxygen non-stoichiometry (δ) of the GDC 10, GDC 20, and GYBC by calculation based on the TGA results at 25-1000 °C. We calculated the δ values from TGA analysis to illustrate the non-stoichiometric oxygen expression due to weight changes, as shown in the figure below. The TGA measurements were conducted in an air atmosphere, and δ values were calculated using the following equation:

$$\Delta\delta = \frac{M_i}{15.999}\left(1 - \frac{m}{m_i}\right)$$

where M_i is the molecular weight of each material; m_i and m are the initial and final weights of the sample upon heating, respectively; and 15.999 g mol^{-1} is the atomic weight of oxygen. As a result, we observed that GYBC demonstrates a superior δ value over time compared to GDC 10 and GDC 20.

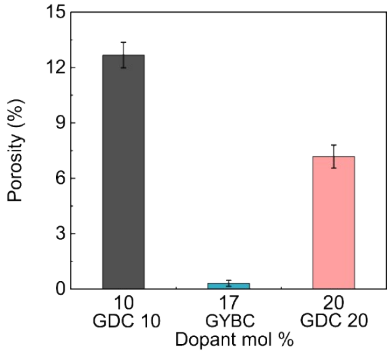

Fig. S5 Porosity measured by the Archimedes method after the sample was pelletized and sintered at 1250 ^{o}C for 2 h. The Archimedes method was used to measure 12 disk pellets and the average value was plotted on the graph and shown as an error bar. The lowest porosity of 0.31% was recorded by GYBC, followed by GDC 20 at 7.2% and GDC 10 at 12.7%.

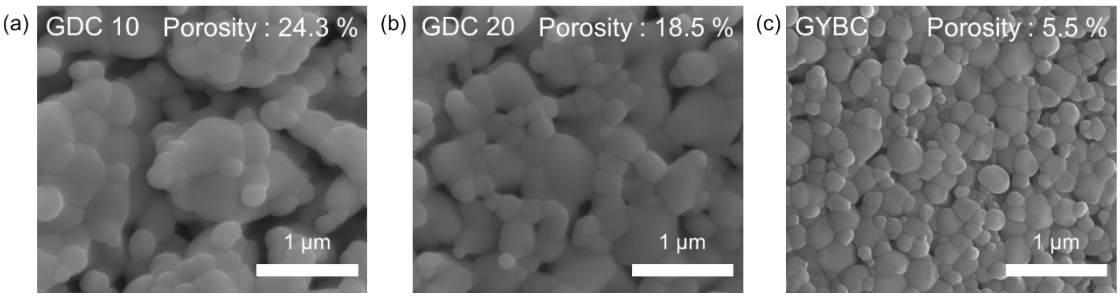

Fig. S6 Surface microstructure of pellets sintered at 1250 ^{o}C for 2 h with (a) GDC 10, (b) GDC 20, and (c) GYBC. The porosity of the surface was calculated by Image J software. The results of surface microstructure show that GYBC (5.5 %) has a lower porosity than that of GDC 10 (24.3 %) and GDC 20 (18.5%). The high sinterability of GYBC contributes to the formation of dense microstructures with well-formed grain-to-grain necking.

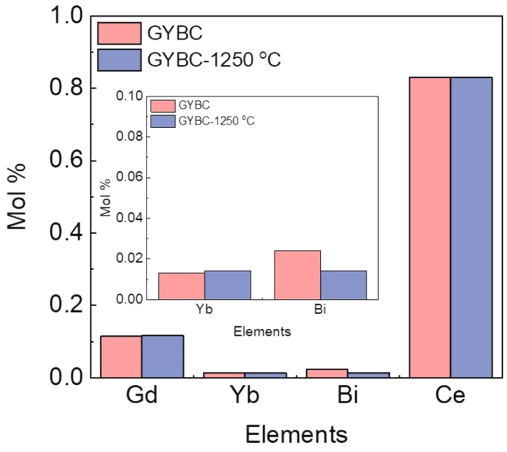

Fig. S7 Inductively coupled plasma–optical emission spectroscopy (ICP-OES) results of GYBC powder before and after sintering at 1250 °C for 2 h. GYBC shows that the Gd and Yb ratios remained largely unchanged after sintering at 1250 °C for 2 h, although some Bi content decreased. This decrease suggests that part of the Bi promoted sintering, while some remained within the GYBC lattice.

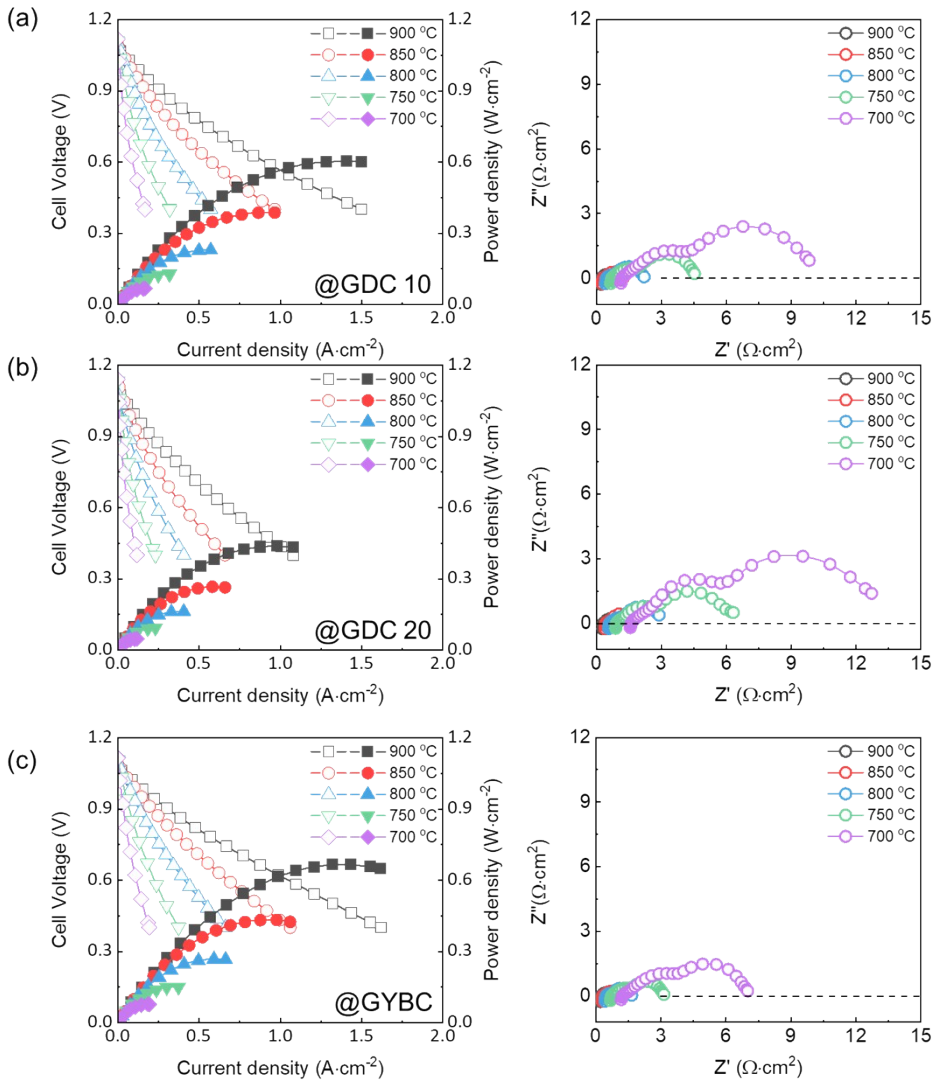

Fig. S8 Electrolyte supported cell (ESC) cell results of I-V curves and impedance spectra (a) GDC 10, (b) GDC 20, and (c) GYBC cell. The maximum power density decreased in the order of GYBC (0.268 W cm^{-2}) > GDC 10 (0.230 W cm^{-2}) > GDC 20 (0.163 W cm^{-2}) at 800 °C. The MPD values for the GYBC cell were recorded at 0.433, 0.268, and 0.151 W cm^{-2} at 850°C, 800°C, and 750°C, respectively. These values indicate a higher performance compared to the GDC 10 and GDC 20 cells. The ohmic resistances of the three cells were similar, but the GYBC cell showed a low polarization resistance of 0.69, 1.19 and 2.41 Ω cm^2 at 850, 800 and 750 °C. It is suggested that the high performance of the GYBC cell is due to its improved electrochemical reaction.

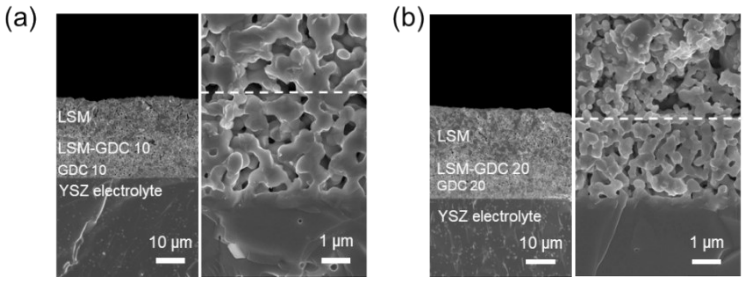

Fig. S9 Cross-sectional microstructure of ESCs (a) GDC 10 cell and (b) GDC 20 cell. The microstructure results show that the GDC 10 and GDC 20 buffer layers are formed with a uniform thickness of 2-3 um, and the respective cathodes are also formed with the same thickness.

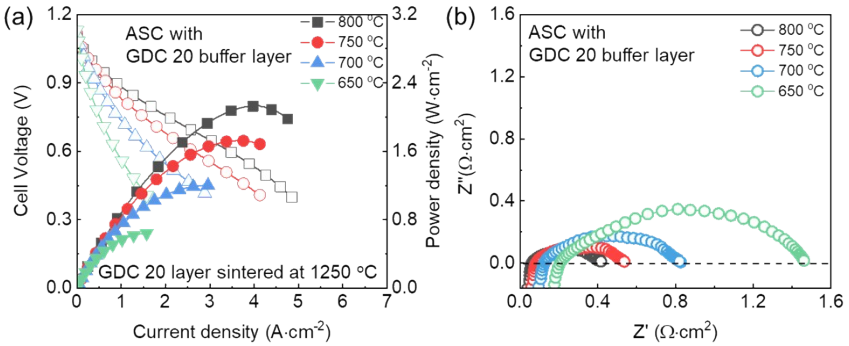

Fig. S10 (a) I-V curves and (b) impedance spectra for the anode-supported cell (ASC) using GDC 20 layer sintered at 1250 °C. The ASC with a GDC 20 buffer layer achieved maximum power densities of 2.47, 2.14, and 1.72 W cm^{-2} at 850, 800, and 750°C, respectively.